Clim. Past Discuss., 11, 5509–5548, 2015
www.clim-past-discuss.net/11/5509/2015/
doi:10.5194/cpd-11-5509-2015

Climate of the Past Discussions

Climatic and insolation control on the high-resolution total air content in the NGRIP ice core

O. Eicher, M. Baumgartner, A. Schilt, J. Schmitt, J. Schwander, T. F. Stocker, and H. Fischer

Climate and Environmental Physics, Physics Institute and Oeschger Centre for Climate Change Research, University of Bern, 3012 Bern, Switzerland

Received: 9 October 2015 – Accepted: 5 November 2015 – Published: 20 November 2015

Correspondence to: O. Eicher (eicher@climate.unibe.ch)

Published by Copernicus Publications on behalf of the European Geosciences Union.

Abstract

Because the total air content (TAC) of polar ice is directly affected by the atmospheric pressure, its record in polar ice cores was considered as a proxy for past ice sheet elevation changes. However the Antarctic ice core TAC record is known to also contain an insolation signature, although the underlying physical mechanisms are still a matter of debate. Here we present a high-resolution TAC record over the whole North Greenland Ice Core Project ice core, covering the last 120 000 years, which independently supports an insolation signature in Greenland. Wavelet analysis reveals a clear precession and obliquity signal similar to previous findings on Antarctic TAC, with different insolation history. In our high-resolution record we also find a decrease of 3–5 % (3–4.2 mL kg^{-1}) in TAC as a response to Dansgaard-Oeschger-Events (DO-events). TAC starts to decrease in parallel to increasing Greenland surface temperature and slightly before CH_4 reacts to the warming, but also shows a two-step decline that lasts for several centuries into the warm phase/interstadial. The TAC response is larger than expected considering only local temperature and atmospheric pressure as a driver, pointing to transient firnification response caused by the accumulation-induced increase in the load on the firn at bubble close-off, while temperature changes deeper in the firn are still small.

1 Introduction

The total air content (TAC) in ice cores from polar regions is one of the many parameters that inform about past environmental conditions. There was hope that TAC would give robust information about the past surface elevation of ice sheets (Lorius et al., 1968), due to its pressure and, thus, altitude dependence. Later, Martinerie et al. (1992) discovered an empirical relationship of pore volume at bubble close-off and snow temperature owing to changes in the densification process in equilibrium conditions. The positive correlation was found mainly in Antarctic, but also alpine and Greenland ice

cores in late Holocene snow. Krinner et al. (2000) and other studies showed that interpreting TAC as an elevation proxy is limited by secular variations in surface pressure as well as by porosity and temperature changes.

More recently Raynaud et al. (2007); Parrenin et al. (2007) and Lipenkov et al. (2011) reported an apparent local summer insolation imprint in TAC and used it to constrain an absolute timescale of Antarctic ice core records. This orbital synchronization is further supported by variations, in the O_2/N_2 ratio, which also dependends on summer insolation (Bender, 2002). Local summer insolation changes are apparently affecting snow surface properties like structure or grain size that remain preserved through firnification down to the pore closure depth.

Grain size in the uppermost 4 m depends on insolation (J. Freitag, personal communication, 2015), but also on daily weather events. Hutterli et al. (2009) state that the total temperature gradient metamorphism (tTGM) influences the physical properties of the snow pack. tTGM is not necessarily synchronous with insolation, leading to a lag between the orbital parameters and the proxies depending on snow structure. How surface snow structure might survive the recrystallization process in the firn is unclear. In view of this on-going discussion and of the fact that a clear insolation effect has so far only been documented in Antarctic ice cores, an independent validation based on Greenland ice which has a different insolation history, is of great importance.

In this paper we present a high-resolution TAC record from the North Greenland Ice Core Project (NGRIP) ice core with 1688 new data points from 134 to 3082 m depth. The aim of this work is twofold. First, to test known influences on TAC, such as the orbital insolation effect observed in Antarctica, for the first time in Greenland. Second, to document transient temperature effects due to rapid temperature changes known as Dansgaard-Oeschger-Events (DO-events) on TAC. Note in this respect that the pore volume effects described above represent a signal imprinted on the firn structure during densification and thus are a signal imprinted in the ice matrix. In contrast, variations in TAC due to direct temperature changes as expected during DO-events reflect changes

in the number density of gas molecules in the pores at bubble close-off and thus are imprinted in the gas record itself.

The paper is organized as follows. Section 2 presents the methods used to derive TAC and the calibration between different measuring periods. In Sect. 3 the new record is shown and compared to data from GRIP, a Greenland ice core located 316 km south-southeast of the NGRIP site. In Sect. 4 we present our results, first we investigate the insolation and non-thermal influences on TAC and perform spectral analysis on our data. In the second part we study the higher-frequency (centennial to millennial) influences on TAC, including the behaviour of TAC during DO-events.

2 Methods

Following Martinerie et al. (1992), the TAC results are expressed in mL kg^{-1} STP and are related to temperature, pore volume and pressure via (Martinerie et al., 1992):

$$V = V_c \frac{P_c \cdot T_0}{T_c \cdot P_0}, \quad (1)$$

with V_c the pore volume, P_c the pressure and T_c the temperature at bubble close-off, P_0 the standard pressure (1013 hPa) and T_0 the standard temperature (273 K).

2.1 Measuring the total air content

The TAC measurements presented here represent a by-product of CH_4 and N_2O concentration measurements performed over many years on the same samples (Flückiger et al., 2004; Huber et al., 2006; Schilt et al., 2010a, 2013; Baumgartner et al., 2012, 2014). To extract the air from the ice samples, the samples are melted in an evacuated vessel. We then refreeze the melt water slowly from below to expel dissolved gases (see e.g. Flückiger et al., 2004). The extracted gas is then expanded into a known volume (Fig. 1). The total air content (TAC) is defined as the volume of air V_0 at standard

temperature T_0 and pressure p_0 per mass m of ice. So:

$$\mathrm{TAC} = \frac{V_0}{m} = \frac{n \cdot R \cdot T_0}{m \cdot p_0} = \frac{R \cdot T_0}{m \cdot p_0} \cdot (n_1 + n_2). \quad (2)$$

In our apparatus, the total amount of gas $n = n_1 + n_2$ is split between two volumes V_1 and V_2, the volume of the sample container and the sampling loop, respectively. $V_1 = V_h + V_t$ is at temperature T_1, which is actually not a homogeneous temperature over V_1, since V_h is cooled below the freezing point while the tubing from the vessel to the sampling loop V_t is exposed to ambient temperatures. T_1 is therefore close to the freezing point, but could not be measured directly. Instead it is assumed to be 275.15 K in a calibration with NEEM ice and data from the Laboratoire de Glaciologie et Géophysique de l'Environnement in Grenoble, as described in the Supplement of NEEM community members (2013). The temperature T_2 in the sampling loop is held constant at $-60 \pm 0.5\,^{\circ}\mathrm{C}$. V_1 is corrected for the small vessel-specific differences, assuming an ice density of $\rho_{\mathrm{ice}} = 917\,\mathrm{kg\,m^{-3}}$. The expanded gas stabilizes in the volume $V_1 + V_2$ at the expansion pressure p_{exp}. With

$$p_{\mathrm{exp}} = \frac{n_1 \cdot R \cdot T_1}{V_1} = \frac{n_2 \cdot R \cdot T_2}{V_2}. \quad (3)$$

Substituting this in Eq. (2) we get:

$$\mathrm{TAC} = \frac{T_0 \cdot p_{\mathrm{exp}}}{m \cdot p_0} \cdot \left(\frac{V_1}{T_1} + \frac{V_2}{T_2} \right). \quad (4)$$

The NGRIP data from 2010, 2011 and 2012 is calculated with Eq. (4), while data from 2002 and 2004 were measured differently. More on this in the next section. Note that the parameter T_1 may slightly vary with lab temperature and also with different extraction vessels. Assuming errors of 0.5 °C for T_1 and T_2, 0.2 mL for V_1 and V_2 and 0.01 g for the mass m, the resulting uncertainty in TAC is $1.3\,\mathrm{mL\,kg^{-1}}$. In the following section the final intercalibration for the whole data set is described.

2.2 Calibration of the air content

The North Greenland Ice Core Project (NGRIP) air content data presented here, stem from different measuring periods and slightly different measuring procedures. The melt-refreeze step was part of all measurements, but the data from 2002 and 2004 were measured as described in Flückiger et al. (2004). The main difference is that the ambient air evacuation step lasted two hours instead of about 30 min and the released air was expanded three times in sequence into a smaller, unchilled sampling loop for analysis. For those measurements the TAC was determined via pressure three times per sample and the analytical error of TAC was estimated as the standard deviation of the three measurements. 287 of the 1626 TAC values were measured following this procedure. The newer (2010–2012) data were measured with a 30 min evacuation step and one injection in a three times larger sampling loop, according to Schilt et al. (2010b). The error is determined by reproducibility measurements. Five randomly distributed, adjacent samples were measured at 15 depths over the different extraction vessels and duration of the measurement series. The pooled standard deviation of the residuals of the 75 samples is $2.20 \pm 0.83\,\mathrm{mL\,kg^{-1}}$, which is higher than the calculated analytical error of $1.3\,\mathrm{mL\,kg^{-1}}$. This is expected due to natural variations of TAC in the ice along the 25 cm and variations in the number and size of the air bubbles opened on the sides of the ice cube during cutting. In order to minimize the latter effect, we cut all samples the same way, in pieces of ~ 40 g.

The 2002/2004 and 2010–2012 data are slightly offset from each other, so a method to intercalibrate was developed. Data pairs of measuring periods we want to compare were identified. Then, the measuring period of 2012 was taken as a reference. Adjacent data from different measuring periods were compared. Only the data from 2010 could not be compared directly to 2012 because they cover different sections of the ice core and hence were compared to the 2011 data. Reference data points of one set are compared with interpolated values of the other dataset. The mean of the offset values are displayed in Table 1. It is assumed that the data scattering is distributed normally

and therefore we take the standard error as the error of the offset. The age offsets to the closest points of the reference values are also shown in Table 1. Note that the interpolations are better if the data points are closer together, reflecting the natural variability of TAC in the ice. Finally the data from 2002 were shifted by 3.4 mL kg^{-1}, those from 2004 by 6.1 mL kg^{-1}, and those from 2011 by −2 mL kg^{-1}. The 2010 data are not significantly different (1.2 ± 1.4 mL kg^{-1}) from 2012, so no correction was made. In the following the corrected data are referred to as melt-refreeze data.

We now also compare our data with data from the same ice core but with independent data obtained from other analytical procedures. A few NGRIP TAC samples have also been measured according to Schmitt et al. (2014) with a different system and an absolute precision of 0.5 mL kg^{-1}. They use samples of 160 g and melt them after evacuation, using infrared radiation. The TAC is determined by pressure and temperature measurements of the released air under well controlled conditions. These data are referred to as vacuum-melt data. 42 out of 62 of these additional NGRIP data points lie within 250 yr to our data, and were used for a nearest-neighbour analysis. For this analysis, each point of the vacuum-melt data was compared with at most the two nearest neighbours of the intercalibrated NGRIP data in each time direction, if they were not more than 70 (250) yr apart from each other. The result is −0.7 ± 2.0 mL kg^{-1} (−0.53 ± 2.1 mL kg^{-1}), so the vacuum-melt data and the melt-refreezing data match within error. Note that the TAC vacuum-melt technique was intercalibrated with TAC data from Raynaud et al. (2007) using overlapping TAC time series from the Dome C ice core (see Schmitt et al., 2014 for details). Accordingly, the two NGRIP TAC records are independently tied to the same reference scale of Raynaud et al. (2007).

3 The NGRIP TAC record

Our new NGRIP record contains 1688 TAC data points and is shown in Fig. 2 on the AICC2012 gas age scale (Veres et al., 2013), along with $\delta^{18}O_{ice}$. The depth range is

133.81 to 3082.23 m, which corresponds on the AICC2012 timescale for gas age to 294 to 119 555 years.

The whole TAC dataset has a mean value of 93.4 mL kg^{-1} with a standard deviation of 4.5 mL kg^{-1}. The measured TAC data show notable variability which is much larger than the analytical error (see Fig. 2). We infer that a considerable part of the scattering in neighbouring samples seems to results from the small scale variability of the TAC signal in the ice itself. One option to verify this is to check whether the scattering diminishes with depth and therefore decreasing annual layer thickness, as described in Baumgartner et al. (2014). If the scattering is a signal in the ice itself, the standard deviation of the values in the 5 adjacent reproducibility samples should get smaller with increasing depth, since high frequency variations will be smoothed out by increasing time interval per sample. In Fig. 3 the standard deviation over the reproducibility measurements is plotted vs. depth. There is a clear trend to lower scattering with depth, although not with a high correlation coefficient, indicating that part of the scatter is embedded in the ice itself. If we assume most of the scattering to be caused by seasonal cycles, then we average over more cycles with increasing age difference in the 25 cm of the adjacent reproducibility samples. The measured variation should therefore decrease with $1/n$, n being the number of years contained in one sample and the 5 samples in each 25 cm interval provide us with an information on the analytical error according to:

$$\sigma^2_{\text{measured}} = \frac{\sigma^2_{\text{ice}}}{n} + \sigma^2_{\text{analytical}}. \quad (5)$$

Letting n go to infinity we get an independent estimate of our analytical error. In Fig. 3 in the right panel we display the variation in the reproducibility samples vs. $1/n$ with the best linear fit. We get a y intersect (corresponding to $n = \infty$) at 1.4 mL^2 kg^{-2}. Taking the square root this independent estimate leads to an analytical error of 1.2 mL kg^{-1}, very close to the 1.3 mL kg^{-1} we calclulated in Sect. 2.1.

3.1 Comparison to GRIP TAC

Raynaud et al. (1997) presented a lower resolution TAC data set from the GRIP ice core. GRIP is located 316 km south-southeast of NGRIP, at an altitude of 3232 m, compared to 2919 m at NGRIP (Dahl-Jensen et al., 1997). Today there is essentially no temperature difference between NGRIP and GRIP (altitude effect is compensated by latitude). Therefore, there is also no difference in pore volume V_c (Martinerie et al., 1992, more on pore volume in the next section) and because of their geographic proximity, insolation differences are insignificant. Accordingly, assuming the temperature consistency did not change in the past, the only difference influencing the TAC is altitude. The GRIP data mainly cover the Holocene with measurements back to 40.6 kyr BP. They also measured older ice, but the stratigraphy of the deepest GRIP part is disturbed (Raynaud et al., 1997) so we refrain from comparing the NGRIP record to that data. In Fig. 4 we show the TAC from Raynaud et al. (1997), along with our two TAC records (melt-refreeze and vacuum melt) in the time interval 0.2 to 45 kyr BP on gas age. The GRIP and NGRIP data are given on a synchronized ice age scale for the Greenland records (Seierstad et al., 2014). The data show good agreement, with the GRIP TAC being slightly lower. To quantify the difference, each point from GRIP was compared with at most the two nearest neighbours of the NGRIP data in each time direction, if they laid within 250 yr. Up to 11.5 kyr (Holocene) GRIP data were only compared to vacuum-melt data since no melt-refreeze data were available. Holocene GRIP TAC is about $1.7 \pm 0.3\,\mathrm{mL\,kg^{-1}}$ lower than NGRIP and glacial GRIP in the interval 11.5 to 45 kyr is $2.4 \pm 0.3\,\mathrm{mL\,kg^{-1}}$ lower, where the error is the standard error of the mean. This is generally in line with the expectations since a higher altitude at the deposition site should lead to lower TAC. Our results leave, on the brink of significance, room for small relative altitude changes from LGM to Holocene, although other studies (e.g. NGRIP Project Members, 2004) state that the relative altitude changes are believed to be small. The barometric formula, assuming a mean annual temperature of −46 °C (−31.5 °C) for stadial (Holocene) conditions at NGRIP leads to a pressure-

elevation gradient of $\delta P/\delta Z$ = 10.5 hPa/100 m (9.9 hPa/100 m). Ignoring temperature, pore volume and upstream correction, Eq. (1) gives an expected TAC difference of $4.2\,\mathrm{mL\,kg^{-1}}$ ($4\,\mathrm{mL\,kg^{-1}}$) at an average of $90\,\mathrm{mL\,kg^{-1}}$ and NGRIP bubble close-off pressure of 701 hPa. This is more than what we observe in our data. Moreover, in reality the pressure-elevation gradient could be larger (11 to 15 hPa/100 m), as automatic weather stations located in the GRIP area suggest (Raynaud et al., 1997). We can not explain the difference with a specific effect. Some of the difference can potentially be explained by an intercalibration issue between the Raynaud et al. (1997) and Schmitt et al. (2014) data. This effect has been estimated to be smaller than $0.5\,\mathrm{mL\,kg^{-1}}$. However the intercalibration was based on recent measurements on the Antarctic EPICA Dome C ice core and methodological and calibration changes over the last 15 years since Raynaud et al. (1997) published the GRIP data cannot be ruled out. At the moment we are not able to quantitatively explain the difference between measured an theoretical TAC values at GRIP and NGRIP.

4 Results and discussion

4.1 Low-frequency variations in TAC

TAC in Antarctica is known to show an anti-correlation with the integrated local summer insolation (ISI) as shown in Raynaud et al. (2007). The ISI is defined as

$$\mathrm{ISI} = \sum \beta_i (w_i \cdot 86\,400). \quad (6)$$

Where w_i is the daily insolation in $\mathrm{W\,m^{-2}}$ and $\beta_i = 1$ if w_i is over the threshold, evaluated by tuning the correlation between ISI and TAC, and $\beta_i = 0$ otherwise. A similar dependency emerges for our Greenland ice core calculating a local summer insolation for the NGRIP drill site. A maximum correlation between TAC and ISI is found for a threshold of $320\,\mathrm{W\,m^{-2}}$, substantially less than the $380\,\mathrm{W\,m^{-2}}$ used by Raynaud et al. (2007) for

the EPICA Dome C (EDC) Antarctic ice core. The correlation difference between 380 and 320 $W m^{-2}$ is however small and the threshold does not alter the shape of the ISI much. Since the temperature at NGRIP is higher than at EDC a lower threshold for additional energy influencing grain structure seems reasonable.

Martinerie et al. (1992) found an empirical relationship between the pore volume V_c at bubble close-off and the temperature for recent equilibrium densification conditions,

$$V_c = 0.76 \cdot \left(\frac{mL}{K\,kg}\right) \cdot T_s - 57 \cdot \left(\frac{mL}{kg}\right), \quad (7)$$

where T_s is the snow temperature in Kelvin, here assumed to be the same as the temperature at bubble close-off depth. Like in Raynaud et al. (2007), we defined the non-thermal residual term V_{cr} as:

$$V_{cr} = V \cdot \frac{T_c}{P_c} \cdot \frac{P_0}{T_0} - V_c(T_s). \quad (8)$$

Where V is the TAC, T_c and P_c the temperature and pressure at bubble close-off depth. For the temperature at bubble close-off we used the heat conduction model results by Kindler et al. (2013), derived from surface temperature variations determined using the $\delta^{15}N$ thermo-diffusion technique (Severinghaus and Brook, 1999; Lang et al., 1999; Kindler et al., 2013), providing data from 10 to 120 kyr and for the pressure at bubble close-off 701 hPa. T_0 and P_0 are the standard temperature (273 K) and standard atmospheric pressure (1013 hPa). For comparison with the analysis by Raynaud et al. (2007), splines (Enting, 1987) with a 750 year cut-off period (COP) through the inversed an standardized TAC data (isTAC) and the inversed and standardized V_{cr} are shown together with the standardized ISI (sISI) in Fig. 5.

The r^2 between V and V_{cr} for the 750 year COP spline is 0.95, so the temperature effect on firnification processes quantified according to Martinerie et al. (1992) is responsible for only 5 % of the TAC variability, in accordance with Raynaud et al. (2007).

These authors derived an r^2 of 0.86 and estimated the temperature induced TAC variations to 10 %. The strong covariance of TAC and local insolation for both Greenland and Antarctic ice cores provides independent evidence of an ISI effect on pore volume as the temporal evolution of ISI in both hemispheres differs significantly. As can be seen in Fig. 5 the shape of the sISI is highly covariant with the low frequency variations of isTAC and V_{cr}, while higher-frequency variations seem to correlate with temperatures on the ice sheet (see Fig. 2). Note that during the glacial, temperature changes in Greenland are often fast, like DO-events, and a 750 COP Spline through the data filters out some of the variations.

Investigations on the higher frequency variations and TAC relation to climate changes during DO-events are discussed in Sect. 4.3.2. In Table 2 the correlations between the sISI, V_{cr}, T_c and isTAC are shown. For the best linear fit we estimate a sensitivity of TAC on the local integrated summer insolation above 320 $W m^{-2}$ of -0.08 mL W kg^{-1} m^{-2} with an r^2 of 0.3.

Figure 5 shows that the correlation of the ISI and the isTAC fails before about 109 kyr, i.e. at the glacial inception at the end of the Eemian. Raynaud et al. (2007) associated the 100 kyr cycle in the Antarctic EDC TAC record to be driven by surface elevation changes inducing pressure differences. The question arises whether the TAC deviations from the expected insolation effect at the glacial inception in our NGRIP record are also related to ice sheet changes. Models for Greenland ice sheet coverage and surface height in the Eemian show little difference to present. Born and Nisancioglu (2012) estimate at NGRIP a maximum lowering of 200 m in the last glacial maximum (LGM) compared to the Holocene. Using the same calculations as in Sect. 3.1, this would account for a TAC change of 2.4 mL kg^{-1}, while the observed TAC changes at the very end of the TAC record are in the order of 10 mL kg^{-1}.

Note that the correlation breakdown between TAC and ISI mainly comes from two data points (see Fig. 2), at 118.8 and 119.4 kyr with very low TAC, and the robustness is therefore questioned. If we exclude these two points and correlate the sISI with the isTAC from the top only until 109 kyr, r^2 increases to 0.48. However, the absolute

changes in TAC are still larger than expected from altitude changes in models. Additionally, it has to be taken in to account that the dating of the ISI is absolute, while the AICC2012 age scale used in this study is fundamentally based on a ice-flow model and in particular shows younger ages for the lowest part of the ice core, compared to other time scales (Veres et al., 2013), with an uncertainty of around 5000 years in the lowest part of the ice core. Accordingly, if the older part of the TAC record were shifted to somewhat older ages, the correlation would increase further. In summary, an ice sheet altitude effect on TAC in the time interval 110–120 kyr BP is rather unlikely. Instead the strong correlation of TAC with ISI for the record before 110 kyr makes an offset in the AICC2012 age scale relative to insolation by several thousand years at the last glacial inception more likely.

4.2 Spectral analysis

Following Raynaud et al. (2007) we performed a wavelet analysis on the TAC data (Fig. 6). Between 20–70 kyr the obliquity effect on TAC is dominant, while for 80–110 kyr the precession cycle dominates. This is in agreement with the findings for EDC, displayed in the right panel of Fig. 6. Since both Antarctic EDC and Greenland NGRIP TAC show the same pattern of either obliquity or precession dominance, we performed a cross-wavelet analysis between the TAC and the respective local ISIs. This analysis allows us to find common spectral signals in time series (see e.g. Grinsted et al., 2004). (Fig. 7).

Our results for NGRIP support the findings by Raynaud et al. (2007) and Lipenkov et al. (2011) on Antarctic TAC being related to ISI. Both records show coherence in the obliquity and precession bands.

4.3 Higher-frequency influences and DO-events

4.3.1 Relation to dust

Based on recent studies (Freitag et al., 2013) small scale firn density is known to correlate with Ca^{2+} representative of mineral dust concentration. Accordingly, a firnification effect of dust on pore volume has been proposed (Hörhold et al., 2012), which should be most pronounced for stadial/interstadial variations, when dust concentrations changed by a factor of about 15 (Fischer et al., 2007). In Fig. 8 the NGRIP TAC, dust (Ruth, 2007), CH_4 and $\delta^{18}O_{ice}$ records are shown on the depth scale for selected DO-events. No simple correlation from TAC to the dust concentration can be observed. During phases when dust concentration is high (e.g., before DO-event 4) TAC varies not differently from when dust is low (e.g. during DO-event 19). Moreover, the TAC variations on their depth scale are not in phase with dust, as would be expected from a direct firnification effect of dust concentrations in the ice matrix on pore volume at bubble close-off. Surprisingly, TAC seems to change more in parallel with CH_4 (anti-correlated) and therefore on gas age scale in the higher-frequency variations, suggesting a direct influence of gas temperature on the number of moles of air enclosed in the pore volume during bubble close-off.

4.3.2 Relation to climate changes during DO-events

The TAC data (Fig. 2) not only show low-frequency variations as discussed in Sect. 4.1 but reveal a strong high-frequency signal. Making use of the unprecedented resolution of our record, we investigate the high-frequency variations and take a closer look on what happens to the TAC during DO-events.

The temperature effect (Eq. 7) on the pore volume would lead to a very small increase in pore volume with rising temperatures. Using the ideal gas we obtain:

$$\mathrm{TAC} = V_{\mathrm{mol}} \cdot n = V_{\mathrm{mol}} \cdot \frac{P_{\mathrm{a}} \cdot V_{\mathrm{c}}(T)}{R \cdot T_{\mathrm{s}}} = \frac{P_{\mathrm{a}} \cdot V_{\mathrm{mol}}}{R} \cdot \left(0.76 - \frac{57\,\mathrm{K}}{T_{\mathrm{s}}}\right). \quad (9)$$

Where V_{mol} is the volume of one mol at STP, $V_c(T)$ the pore volume at close off, R is the gas constant 8.31 J mol^{-4} kg^{-1}, T_s the snow temperature and n the number of moles of air enclosed in the bubbles. Therefore, a slight increase in TAC with increasing temperature is expected from the pore volume effect. However, the formula for pore volume changes, derived in Martinerie et al. (1992) from steady state Holocene conditions is most likely not applicable during DO-events where a transient change in densification occurs. It is reasonable to assume the pore volumes in the firn does not follow the temperature (Eq. 7) directly at the onsets of DO-events. If we assume that the pore volume remains constant in the first stage of a DO-event, the first-order effect of slowly increasing temperatures in the firn would lead then to a decrease in TAC, what our data (Fig. 2) seem to support. It is possible that pore volume even decreases at the beginning of a DO-event as will be discussed in the next chapter. To test objectively whether there is a correlation of decreases in TAC with DO-events we developed a method to find significant decreases. To remove noise in the TAC raw data 1000 Monte Carlo splines with a cut-off period of 750 years were calculated on the AICC2012 gas age scale, and the mean of the 1000 splines was taken as our best-guess representation of true TAC variations (Monte Carlo Average, MCA). This MCA-spline is then searched for maxima and minima. A detected minimum is considered significant if the difference between the last maximum and the minimum is larger than 1.5 times the added standard deviation of the spline at both points. The result is shown in Fig. 9. With these criteria and parameters the routine finds 23 significant minima, out of which 17 are related to a DO-event in $\delta^{18}O_{ice}$. The significant minima unassociated with a DO-event occur during the Younger Dryas, two in the LGM and one during DO-event 25. There is another one before DO-event 24, which is due to a wiggle in the spline fit, leading to two significant minima in the descent preceding DO-event 24 (see Fig. 9). Using the above mentioned parameters, the routine fails to find significant minima related to DO-events 8, 9, 16–18, 20, 22, 23 and 25, although, for many of these cases there exists a decline in TAC, which, however, did not satisfy our significance criterion. For DO-events 9, 18 (and the event p18, not a full DO, but preceding DO-event 18), 20, 23 and 25 this is

due to the threshold of 1.5 σ being too high, while 16–17 follow each other very closely so the TAC response signal might not be visible. For DO-event 22 the minimum is more than a thousand years before the $\delta^{18}O_{ice}$ maximum, so we considered this not to be related to the warming. DO-event 22 has a small amplitude in $\delta^{18}O_{ice}$ compared to the background and the other DOs. For DO-event 8 the TAC data scatters a lot.

Interesting is also the timing of the TAC minima compared to the maxima in the $\delta^{18}O_{ice}$. In Table 3 the timing of the minima in TAC on the AICC2012 gas age scale and the maxima in the rises of $\delta^{18}O_{ice}$ on the AICC2012 ice age scale are shown. On average the TAC change is synchronous within the error (12 ± 290 years). Due to the considerable analytical and small scale scatter of our TAC data it is difficult to pinpoint the temporal evolution of the TAC and its phase relationship to other climate proxies in the ice core for individual DO-events. Moreover, when comparing $\delta^{18}O_{ice}$ in the ice matrix and a direct temperature related signal in TAC, the uncertainty in the ice age-gas age difference has to be taken into account.

To figure out how the TAC reacts in general to DO-event warmings, we calculated a stack of TAC variations during DO-events and compared it to other gas phase parameters. Since the TAC seems to react in the time window where also the CH_4 shows changes, we stacked the TAC around the onsets in CH_4. For this we defined a criterion for the rise in CH_4. The analytical error in the CH_4 data is 5.9 ppbv, according to Baumgartner et al. (2014). The start of the CH_4 increase was defined in the middle between the first two data points during the onset of stadial/interstadial transitions which did not agree anymore within their 2 σ uncertainty on the AICC2012 gas age scale. This criterion gives the onsets seen in Table 4. Only for DO-event 2, no significant time point could be defined. The same stacking analysis was performed for $\delta^{15}N$ (Kindler et al., 2013) indicating temperature gradients across the firn column, which are controlled by rapid warming at the surface. The TAC (this study) and the $\delta^{15}N$ from Kindler et al. (2013) were then cut out in age windows +200 and −1000 years around the DO-onsets in CH_4. For each window we subtracted the mean value over this time span to remove the long term trend in the data. Note that we neglected the tempera-

ture effect on pore volume as discussed in Sect. 4.1, as this effect is small (Fig. 5) and does not occur in the gas itself but acts on the firn matrix. Due to the ice age/gas age difference, the latter process is, therefore, not in phase with changes in temperature but affects TAC several hundred years later. The resulting data were then stacked and for each, the CH_4, the TAC, and $\delta^{15}N$ data a spline with a COP of 200 years was calculated. The result is displayed in the left panel of Fig. 10. Relative to CH_4, the measured TAC decrease starts around 100 years earlier. Within the error, the $\delta^{15}N$ starts to increase synchronously with TAC. This 100 year lag of CH_4 to temperature is somewhat more than the 25–70 ± 25 years calculated for DO-events in Marine Isotope Stage 3 in previous studies (Huber et al., 2006), and clearly more than 4.5^{+21}_{-24} years for the Bølling-Allerød (BA) calculated in Rosen et al. (2014). This difference can partly be attributed to our method, to detect the onset of the stadial/interstadial change, as we focussed on TAC anomalies and not on the exact timing of the CH_4 rises. Note that the stacked TAC data show a two-step decrease that lasts over several hundred years. When the $\delta^{15}N$ signal reaches its maximum, TAC is still decreasing, shortly before the $\delta^{15}N$ stabilizes the TAC slightly rises and then drops in a second step to lower values than before the event. Within the error TAC and $\delta^{15}N$ start to change synchronously, indicating a direct surface temperature effect on TAC.

The total amplitude of the TAC's response is $-3.6 \pm 0.6\,mL\,kg^{-1}$. Using Eq. (1) with all parameters but the temperature fixed, we can calculate the expected physical TAC response according to the ideal gas law (Fig. 10b). The temperature influencing the TAC is the bubble close-off temperature, as derived by Kindler et al. (2013) using a heat transport model with the surface temperature determined by $\delta^{15}N$ thermodiffusion thermometry. To get an average behaviour of bubble close-off temperature, we also stacked the modelled firn temperature at bubble close-off for the DO-events in windows of +200 to −800 years relative to the onset in CH_4. We then calculated the mean over 50 yr intervals from +175 to −775 yr around the starting points of the bubble close-off warmings (red points in Fig. 10b). With a starting temperature and TAC of 227.15 K and $90\,mL\,kg^{-1}$, respectively, we computed the expected TAC response (blue crosses

in Fig. 10b). Also shown in Fig. 10b are the measured TAC values on ice age scale for comparison with the modelled TAC and the temperature at the surface. The calculated amplitude of the direct temperature effect through the ideal gas law (number density of molecules per volume) at bubble close-off is $1.4\,mL\,kg^{-1}$, which is significantly smaller than the measured one. The amplitude difference indicates that other effects than the temperature at bubble close-off influence TAC on short timescales and especially during the second step of the TAC decrease, where in situ gas temperature changes are already quite small. Also TAC changes simultaneously with surface temperature, confirming the previous results but indicating again that temperature is not sufficient to explain the TAC changes later during a DO-event. One possibility, to explain the larger TAC amplitude than expected from the direct temperature effect, could be co-occurring changes in surface pressure for example related to synoptic pressure pattern changes related to DO-events.

To explain the full amplitude in DO-event TAC changes, however, a pressure decrease at the NGRIP site of around 17 hPa would be required during interstadial warmings. This could be related to a northward shift of North Atlantic storm tracks (Kageyama et al., 2009) connected to a drastic reduction of sea ice during DO-events, which would also lead to a lowering of synoptic pressure over Greenland (Zhang et al., 2014). However, compared to currently observed spatial gradients in mean annual sea level pressure over the North Atlantic the size of this effect appears too large and, moreover, should occur synchronously to the onset of the DO-events. In contrast a transient effect of changes in firnification, hence pore volume, during Greenland interstadials appears more likely to explain our observations. We suggest that such an effect can be induced by the rapidly increasing accumulation rate at the onset of the DO-event. This leads to a higher load and thus enhanced deformation of the snow grains at depth at a time when the temperature in the firn column is still cold. A simple transient firnification model experiment (Sect. 4.3.3) supports this conclusion by reducing TAC by several $mL\,kg^{-1}$ as in our observations.

4.3.3 Transient firnification model experiment

Empirical equations for estimating bubble close-off densities and bubble close-off depths have been derived for steady state conditions (Martinerie et al., 1992, 1994). Especially at the beginning of a DO-event the firn layer is far from being in a steady condition. Fast artificial sintering of snow by applying high pressures results in very low TAC compared to natural firnification (B. Stauffer, personal communication, 2015). The reason for low TAC in artificially sintered ice is most likely that there is not enough time to form spherical cavities, which are a result of minimizing surface energy by slow mass redeposition by vapor diffusion. We therefore expect that after a step-like increase in accumulation rate at the beginning of a DO-event the additional pressure in the bubble close-off zone caused by the increasing load of snow leads to expelling air from open pores yielding lower TAC, compared to steady state conditions. We estimate the upper limit of this effect by assuming that for some 140 annual layers above the firn-ice transition the time required to reach bubble close-off remains unchanged after a transition into a DO-event. This assumption is based on the fact that the temperature at the depth of bubble close-off remains near the cold state during the first 140 years of a DO-event (less than 20 % response to the surface temperature change, Fig. 10) and on the hypothesis that time is more important for finalizing the firnification process bubble close-off than the additional hydrostatic pressure.

We modelled the firn density during the transition into a DO-event with a transient firnification model (Schwander et al., 1997). Interstadial temperature is set to −46 °C and ice accumulation rate to 0.05 m a^{-1}. At the beginning of the simulated DO-event we increase the temperature to −36 °C and the ice accumulation rate to 0.1 m a^{-1} within 100 years. We have calculated the density of the layer with the age corresponding to the bubble close-off age under steady state interstadial conditions. This density is assumed to be the bubble close-off density during the first part of the event. The resulting TAC of the simulation is shown in Fig. 11. We interpret the decrease in TAC as the extreme scenario for the first 140 years of a DO-event. The real effect might be smaller.

Later, when the temperature at the firn-ice transition increases further, TAC will slowly approach the new equilibrium value. As there is no physical model describing this dynamic behavior yet, we cannot provide a more precise development of TAC during a DO-event, but the decrease in TAC as observed in the NGRIP ice core seems to be compatible with the simulation.

5 Conclusions

We present the first high-resolution TAC record from the Greenland NGRIP ice core covering the last 120 kyr. In line with previous studies in Antarctica (Raynaud et al., 2007; Lipenkov et al., 2011) we find the low frequency variations to depend on local summer insolation and thus the orbital parameters. Those effects act on the firn matrix controlling the pore volume during bubble close-off and, thus, operate on the ice age scale, (e.g. Raynaud et al., 2007; Bender, 2002), although the origin of this process is not yet clear. Additionally, in steady-state, the pore volume is known to correlate with firn temperature (Martinerie et al., 1992), which is also an ice property leading to TAC changes. Our studies show that this temperature effect imprinted on pore volume during densification in steady state is small compared to the insolation effect operating at the surface, and also small compared to a direct temperature effect on TAC imposed by the change in mole density of the gas during bubble enclosure that we clearly observe during DO-events.

Comparison of δ^{15}N, CH_4 and TAC, all on the gas age scale, provides evidence that surface temperature warming, or an effect synchronous to surface warming, has a direct imprint on the TAC. The immediate decrease in TAC at an onset of a DO-event could have two possible sources according to the ideal gas law: decreasing air pressure or less amount of substance per volume due to rising temperature. However, both effects appear to be too small to explain the measured TAC decline. Large changes in the height of the ice sheet are ruled out for such very short term variations as the TAC change occurs immediately during the DO-event warming, while the ice sheet response

would be slow and delayed. However, the increasing accumulation rate during DO-events leads to an increase in firn thickness of several tens of meters, which through the additional weight on the firn column leads to a temporarily enhanced densification. This could reduce TAC for several centuries after the onset of the DO-event. After 500–1000 years the firn column reaches a new equilibrium with ambient temperature, accumulation and pore volume and TAC reaches again its steady state value.

With the TAC signal being influenced by effects on the ice age and gas age scale, this also limits the precision of deriving orbital timescales from TAC as done e.g. by Lipenkov et al. (2011). Moreover, the processes that connect surface insolation changes with the pore volume changes at the bubble close-off depth are not yet understood. Therefore we refrain from using TAC in Greenland for orbital tuning.

Acknowledgements. Continuing support by the Swiss National Science Foundation for ice core research at the University of Bern is gratefully acknowledged. NGRIP is coordinated by the Department of Geophysics at the Niels Bohr Institute for Astronomy, Physics and Geophysics, University of Copenhagen. It is supported by Funding Agencies in Denmark (SHF), Belgium (FNRS-CFB), France (IPEV and INSU/CNRS), Germany (AWI), Iceland (RannIs), Japan (MEXT), Sweden (SPRS), Switzerland (SNF) and the USA (NSF, Office of Polar Programs). We thank J. Freitag for fruitful discussion on firnification and bubble enclosure processes.

References

Baumgartner, M., Schilt, A., Eicher, O., Schmitt, J., Schwander, J., Spahni, R., Fischer, H., and Stocker, T. F.: High-resolution interpolar difference of atmospheric methane around the Last Glacial Maximum, Biogeosciences, 9, 3961–3977, doi:10.5194/bg-9-3961-2012, 2012. 5512

Baumgartner, M., Kindler, P., Eicher, O., Floch, G., Schilt, A., Schwander, J., Spahni, R., Capron, E., Chappellaz, J., Leuenberger, M., Fischer, H., and Stocker, T. F.: NGRIP CH_4 concentration from 120 to 10 kyr before present and its relation to a $\delta^{15}N$ temperature reconstruction from the same ice core, Clim. Past, 10, 903–920, doi:10.5194/cp-10-903-2014, 2014. 5512, 5516, 5524

Bender, M. L.: Orbital tuning chronology for the Vostok climate record supported by trapped gas composition, Earth Planet. Sc. Lett., 204, 275–289, 2002. 5511, 5528

Born, A. and Nisancioglu, K. H.: Melting of Northern Greenland during the last interglaciation, The Cryosphere, 6, 1239–1250, doi:10.5194/tc-6-1239-2012, 2012. 5520

Dahl-Jensen, D., Gundestrup, N., Keller, K., Johnsen, S., Gogineni, S., Allen, C., Chuah, C., Miller, H., Kipfstuhl, S., and Wassington, E.: A search in north Greenland for a new ice-core drill site, J. Glaciol., 43, 300–306, 1997. 5517

Enting, I. G.: On the use of smoothing splines to filter CO_2 data, J. Geophys. Res.-Atmos., 92, 10977–10984, 1987. 5519, 5539

Fischer, H., Siggaard-Andersen, M.-L., Ruth, U., Röthlisberger, R., and Wolff, E.: Glacial/interglacial changes in mineral dust and sea-salt records in polar ice cores: sources, transport, and deposition, Rev. Geophys., 45, rG1002, doi:10.1029/2005RG000192, 2007. 5522

Flückiger, J., Blunier, T., Stauffer, B., Chappellaz, J., Spahni, R., Kawamura, K., Schwander, J., Stocker, T., and Dahl-Jensen, D.: N_2O and CH_4 variations during the last glacial epoch: insight into global processes, Global Biogeochem. Cy., 18, doi:10.1029/2003GB002122, 2004. 5512, 5514

Freitag, J., Kipfstuhl, S., Laepple, T., and Wilhelms, F.: Impurity-controlled densification: a new model for stratified polar firn, J. Glaciol., 59, 1163–1169, doi:10.3189/2013JoG13J042, 2013. 5522

Grinsted, A., Moore, J. C., and Jevrejeva, S.: Application of the cross wavelet transform and wavelet coherence to geophysical time series, Nonlin. Processes Geophys., 11, 561–566, doi:10.5194/npg-11-561-2004, 2004. 5521

Huber, C., Leuenberger, M., Spahni, R., Flückiger, J., Schwander, J., Stocker, T. F., Johnsen, S., Landals, A., and Jouzel, J.: Isotope calibrated Greenland temperature record over Marine Isotope Stage 3 and its relation to CH_4, Earth Planet. Sc. Lett., 243, 504–519, 2006. 5512, 5525

Hutterli, M., Schneebeli, M., Freitag, J., Kipfstuhl, J., and Röthlisberger, R.: Impact of local insolation on snow metamorphism and ice core records, Low Temperature Science, 68, 223–232, 2009. 5511

Hörhold, M., Laepple, T., Freitag, J., Bigler, M., Fischer, H., and Kipfstuhl, S.: On the impact of impurities on the densification of polar firn, Earth Planet. Sc. Lett., 325–326, 93–99, doi:10.1016/j.epsl.2011.12.022, 2012. 5522

Kageyama, M., Mignot, J., Swingedouw, D., Marzin, C., Alkama, R., and Marti, O.: Glacial climate sensitivity to different states of the Atlantic Meridional Overturning Circulation: results from the IPSL model, Clim. Past, 5, 551–570, doi:10.5194/cp-5-551-2009, 2009. 5526

Kindler, P., Guillevic, M., Baumgartner, M., Schwander, J., Landais, A., and Leuenberger, M.: NGRIP temperature reconstruction from 10 to 120 kyr b2k, Clim. Past Discuss., 9, 4099–4143, doi:10.5194/cpd-9-4099-2013, 2013. 5519, 5524, 5525, 5547

Krinner, G., Raynaud, D., Doutriaux, C., and Dang, H.: Simulations of the last glacial maximum ice sheet surface climate: implications for the interpretation of ice core air content, J. Geophys. Res.-Atmos., 105, 2059–2070, 2000. 5511

Lang, C., Leuenberger, M., Schwander, J., and Johnsen, S.: 16 °C rapid temperature variation in central greenland 70,000 years ago, Science, 286, 934–937, doi:10.1126/science.286.5441.934, 1999. 5519

Lipenkov, V., Raynaud, D., Loutre, M., and Duval, P.: On the potential of coupling air content and O_2/N_2 from trapped air for establishing an ice core chronology tuned on local insolation, Quaternary Sci. Rev., 30, 3280–3289, 2011. 5511, 5521, 5528, 5529

Lorius, C., Raynaud, D., and Dolle, L.: Densité de la glace et Étude des gaz en profondeur dans un glacier antarctique, Tellus, 20, 449–460, 1968. 5510

Martinerie, P., Raynaud, D., Etheridge, D. M., Barnola, J. M., and Mazaudier, D.: Physical and climatic parameters which influence the air content in polar ice, Earth Planet. Sc. Lett., 112, 1–13, 1992. 5510, 5512, 5517, 5519, 5523, 5527, 5528, 5542

Martinerie, P., Lipenkov, V. Y., Raynaud, D., Chappellaz, J., Barkov, N. I., and Lorius, C.: Air content paleo record in the Vostok ice core (Antarctica): a mixed record of climatic and glaciological parameters, J. Geophys. Res., 99, 10565–10576, 1994. 5527

NEEM community members: Eemian interglacial reconstructed from a Greenland folded ice core, Nature, 493, 489–494, doi:10.1038/nature11789, 2013. 5513

NGRIP Project Members: High-resolution record of Northern Hemisphere climate extending into the last interglacial period, Nature, 431, 147–151, doi:10.1038/nature02805, 2004. 5517, 5539

Parrenin, F., Barnola, J.-M., Beer, J., Blunier, T., Castellano, E., Chappellaz, J., Dreyfus, G., Fischer, H., Fujita, S., Jouzel, J., Kawamura, K., Lemieux-Dudon, B., Loulergue, L., Masson-Delmotte, V., Narcisi, B., Petit, J.-R., Raisbeck, G., Raynaud, D., Ruth, U., Schwander, J., Severi, M., Spahni, R., Steffensen, J. P., Svensson, A., Udisti, R., Waelbroeck, C., and

Wolff, E.: The EDC3 chronology for the EPICA Dome C ice core, Clim. Past, 3, 485–497, doi:10.5194/cp-3-485-2007, 2007. 5511

Raynaud, D., Chappellaz, J., Ritz, C., and Martinerie, P.: Air content along the Greenland Ice Core Project core: a record of surface climatic parameters and elevation in Central Greenland, J. Geophys. Res., 102, 26607–26613, 1997. 5517, 5518, 5541

Raynaud, D., Chappellaz, J., Ritz, C., and Martinerie, P.: The local insolation signature of air content in Antarctic ice. A new step toward an absolute dating of ice records, Earth Planet. Sc. Lett., 261, 337–349, 2007. 5511, 5515, 5518, 5519, 5520, 5521, 5528, 5542, 5543, 5544

Rosen, J. L., Brook, E. J., Severinghaus, J. P., Blunier, T., Mitchell, L. E., Lee, J. E., Edwards, J. S., and Gkinis, V.: An ice core record of near-synchronous global climate changes at the Bolling transition, Nat. Geosci., 7, 459–463, doi:10.1038/ngeo2147, 2014. 5525

Ruth, U.: Dust concentration in the NGRIP ice core, doi:10.1594/PANGAEA.587836, supplement to: Ruth, U., Bigler, M., Röthlisberger, R., Siggaard-Andersen, M.-L., Kipfstuhl, J., Goto-Azuma, K., Hansson, M. E., Johnsen, S. J., Lu, H., Steffensen, J. P.: Ice core evidence for a very tight link between North Atlantic and east Asian glacial climate, Geophys. Res. Lett., 34, L03706, doi:10.1029/2006GL027876, 2007. 5522, 5545

Schilt, A., Baumgartner, M., Schwander, J., Buiron, D., Capron, E., Chappellaz, J., Loulergue, L., Schüpbach, S., Spahni, R., Fischer, H., and Stocker, T. F.: Atmospheric nitrous oxide during the last 140,000 years, Earth Planet. Sc. Lett., 300, 33–43, 2010a. 5512

Schilt, A., Baumgartner, M., Blunier, T., Schwander, J., Spahni, R., Fischer, H., and Stocker, T. F.: Glacial-interglacial and millennial-scale variations in the atmospheric nitrous oxide concentration during the last 800,000 years, Quaternary Sci. Rev., 29, 182–192, doi:10.1016/j.quascirev.2009.03.011, 2010b. 5514

Schilt, A., Baumgartner, M., Eicher, O., Chappellaz, J., Schwander, J., Fischer, H., and Stocker, T.: The response of atmospheric nitrous oxide to climate variations during the last glacial period, Geophys. Res. Lett., 40, 1888–1893, doi:10.1002/grl.50380, 2013. 5512

Schmitt, J., Seth, B., Bock, M., and Fischer, H.: Online technique for isotope and mixing ratios of CH_4, N_2O, Xe and mixing ratios of organic trace gases on a single ice core sample, Atmos. Meas. Tech., 7, 2645–2665, doi:10.5194/amt-7-2645-2014, 2014. 5515, 5518

Schwander, J., Sowers, T., Barnola, J. M., Blunier, T., Malaizé, B., and Fuchs, A.: Age scale of the air in the Summit ice: implication for glacial-interglacial temperature change, J. Geophys. Res., 102, 19483–19494, 1997. 5527, 5548

Seierstad, I. K., Abbott, P. M., Bigler, M., Blunier, T., Bourne, A. J., Brook, E., Buchardt, S. L., Buizert, C., Clausen, H. B., Cook, E., Dahl-Jensen, D., Davies, S. M., Guillevic, M., Johnsen, S. J., Pedersen, D. S., Popp, T. J., Rasmussen, S. O., Severinghaus, J. P., Svensson, A., and Vinther, B. M.: Consistently dated records from the Greenland GRIP, GISP2 and NGRIP ice cores for the past 104 ka reveal regional millennial-scale delta O-18 gradients with possible Heinrich event imprint, Quaternary Sci. Rev., 106, 29–46, doi:10.1016/j.quascirev.2014.10.032, 2014. 5517, 5541

Severinghaus, J. P. and Brook, E. J.: Abrupt climate change at the end of the last glacial period inferred from trapped air in polar ice, Science, 286, 930–934, doi:10.1126/science.286.5441.930, 1999. 5519

Veres, D., Bazin, L., Landais, A., Toyé Mahamadou Kele, H., Lemieux-Dudon, B., Parrenin, F., Martinerie, P., Blayo, E., Blunier, T., Capron, E., Chappellaz, J., Rasmussen, S. O., Severi, M., Svensson, A., Vinther, B., and Wolff, E. W.: The Antarctic ice core chronology (AICC2012): an optimized multi-parameter and multi-site dating approach for the last 120 thousand years, Clim. Past, 9, 1733–1748, doi:10.5194/cp-9-1733-2013, 2013. 5515, 5521, 5539

Zhang, X., Lohmann, G., Knorr, G., and Purcell, C.: Abrupt glacial climate shifts controlled by ice sheet changes, Nature, 512, 290–294, 2014. 5526

Table 1. Table with the offsets between the data from different measuring periods. The second number in the intervals column is the reference period. Offset values are the median of all data points compared. The given error is the standard error. *n* is the number of points compared. Av. age offset denotes the average difference to the closer endpoint of the interpolation interval. The 2010 data could not be compared directly to 2012, so the offset values in the table are calculated from the other offsets.

Intervals [yr]	Offset [mL kg^{-1}]	*n*	Av. age offset [yr]
2004 and 2012	-6.1 ± 0.6	33	196
2002 and 2012	-3.4 ± 2.1	24	348
2010 and 2011	3.2 ± 0.9	37	47
2012 and 2011	-2.0 ± 1.1	24	344
2010 and 2012	1.2 ± 1.4	–	–

Table 2. Table with the correlations between data and calculated parameters. isTAC denotes the inversed standardized TAC, sISI the standardized ISI record, V_{cr} the non-thermal residual term of the pore volume and T_c the standardized temperature at bubble close-off.

	isTAC	sISI	V_{cr}	T_c
isTAC	–	0.30	0.95	0.26
sISI	0.30	–	0.21	0.00

Table 3. Timing of the DO-events in $\delta^{18}O_{ice}$ and TAC. The time value in $\delta^{18}O_{ice}$ denotes the maximum of the rise in $\delta^{18}O_{ice}$ on the AICC2012 ice age scale, defined by eye. The time point in TAC is the time of the minimum, found with the method described in Sect. 4.3.2. On average the $\delta^{18}O_{ice}$ rise is younger by 12 ± 290 years with a median of −10 years.

DO-event	$\delta^{18}O_{ice}$ [AICC2012 ice]	TAC [AICC2012 gas]	Difference
1	11 570	11 580	−10
BA	14 551	14 560	−9
2	23 251	23 600	−349
3	27 691	27 820	−129
4	28 751	28 790	−39
5	32 410	32 660	−250
6	33 630	33 810	−180
7	35 390	35 480	−90
10	41 391	41 220	171
11	43 270	43 140	130
12	46 789	46 610	179
13	49 210	50 020	−810
14	54 151	53 880	271
15	55 651	55 440	211
19	72 087	71 940	147
21	84 130	83 570	560
24	105 747	105 760	−13
		Average	−12 ± 290
		Median	−10

Table 4. Timing of the DO-events in methane. The time value denotes the average time between the first two-sigma increase in CH_4 from its stadial value and the point before, on the AICC2012 gas age scale.

DO-event	CH_4 [AICC2012 gas]	DO-event	CH_4 [AICC2012 gas]
BA	15 041	14	54 295
2	–	15	55 861
3	28 117	16	58 308
4	29 509	17	59 108
5	33 080	18	64 126
6	34 578	19	72 101
7	35 889	20	75 839
8	38 312	21	84 454
9	40 271	22	89 402
10	41 476	23	101 840
11	43 446	24	106 050
12	46 847	25	112 968
13	49 347		

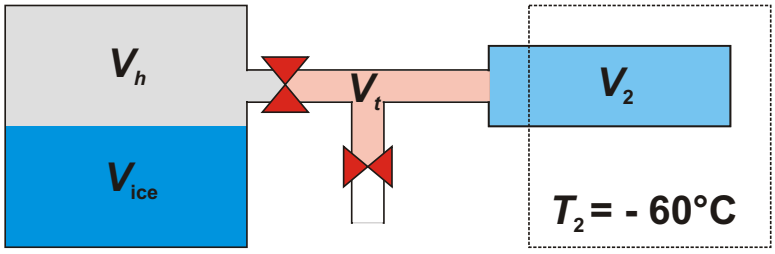

Figure 1. Scheme of the volumes involved in the TAC measurements. The gas from the refrozen melt water in the vessel on the left is confined in the headspace volume V_h. It is then expanded in the Volume $V_{exp} = V_1 + V_2 = V_h + V_t + V_2$. The temperature T_2 in V_2 is held at −60 °C.

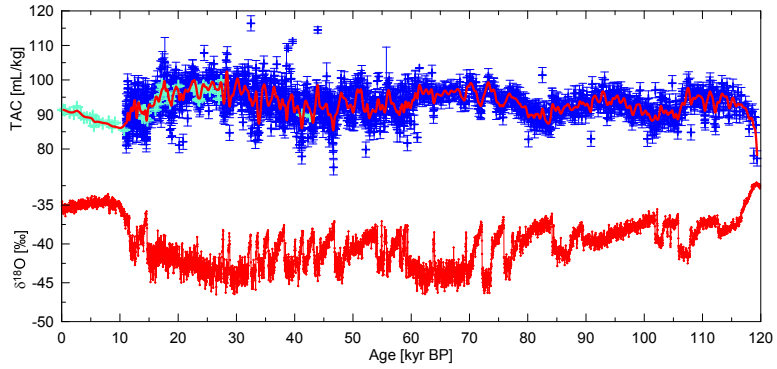

Figure 2. The NGRIP TAC record of this study on the AICC2012 gas age scale (Veres et al., 2013), using two different methods. In blue the melt-refreeze data, in turquoise the vacuum-melt TAC. The red line represents a spline with a 750 yr cut-off period (COP), according to Enting (1987). At the bottom, the $\delta^{18}O_{ice}$ for the NGRIP ice core (NGRIP Project Members, 2004) is given.

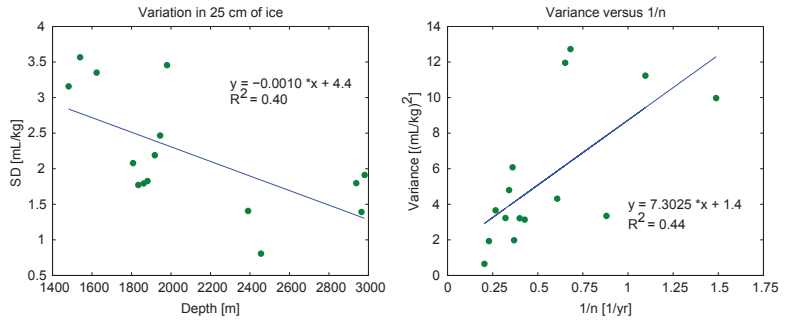

Figure 3. Left: standard deviation of reproducibility measurements in the TAC dependent on depth. Each point represents the mean over 5 adjacent samples. As expected, the variations get smaller with the smoothing due to thinner annual layers. Right: the variation of the reproducibility measurements vs. $1/n$, where n is the number of annual cycles in the sample.

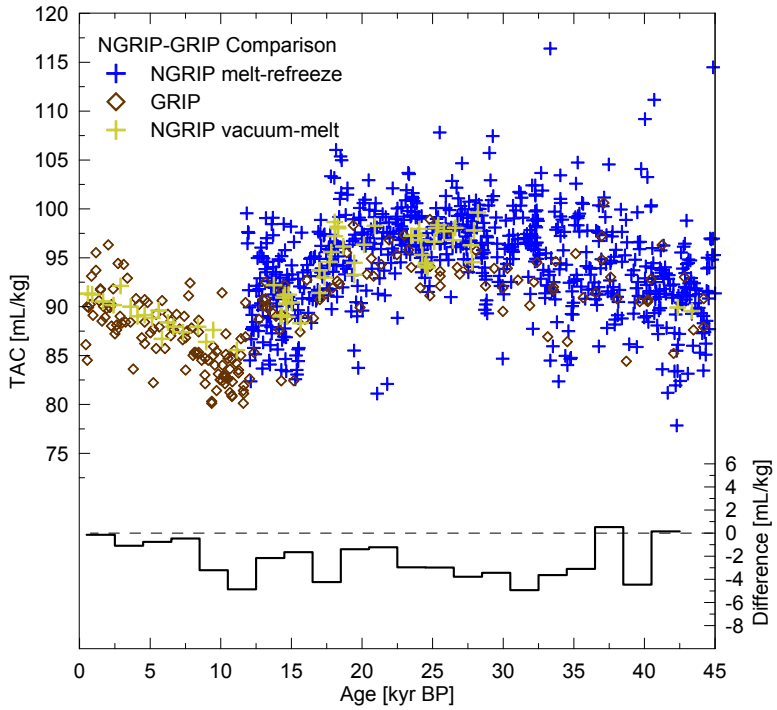

Figure 4. GRIP data (Raynaud et al., 1997) in brown, vacuum-melt TAC data in yellow, melt-refreeze TAC data in blue. All data on the synchronized ice age scale for GRIP and NGRIP, according to Seierstad et al. (2014). The black curve represents the difference between GRIP and NGRIP TAC data in 2 kyr intervals.

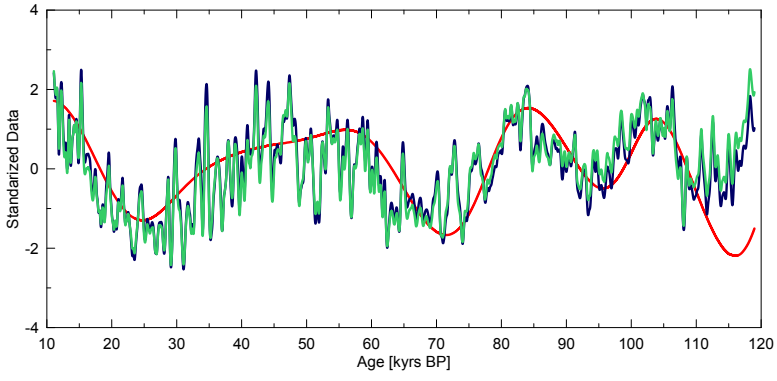

Figure 5. In red the integrated summer insolation sISI on days with more than 320 $W m^{-2}$. In blue a standardized spline with 750 COP of the inversed total air content record. In green, analogous to Raynaud et al. (2007) the standardized TAC data after correcting for the temperature effect on pore volume V_{cr} (Martinerie et al., 1992). Note that the ice core data are on the glaciological AICC2012 ice age scale, while ISI is on an absolute astronomical age scale.

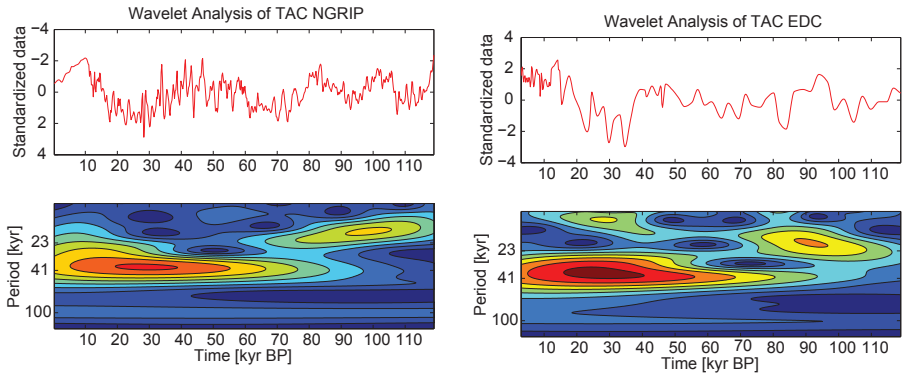

Figure 6. Left: the inversed TAC data in red, re-sampled at an age step of 0.2 kyr and wavelet analysis of this spline. Right: EDC TAC data (Raynaud et al., 2007), re-sampled at 0.2 kyr and its wavelet analysis in the same time window.

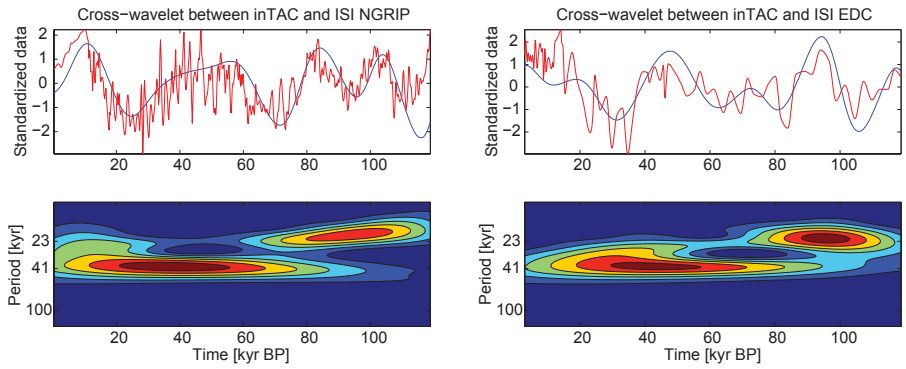

Figure 7. Left: the inversed TAC data, re-sampled at 0.2 kyr in red, sISI with a threshold of 320 $W m^{-2}$ in blue and cross-wavelet analysis thereof. Right: EDC TAC (Raynaud et al., 2007) re-sampled at 0.2 kyr, sISI with a threshold 380 $W m^{-2}$ and cross-wavelet analysis of the EDC and sISI.

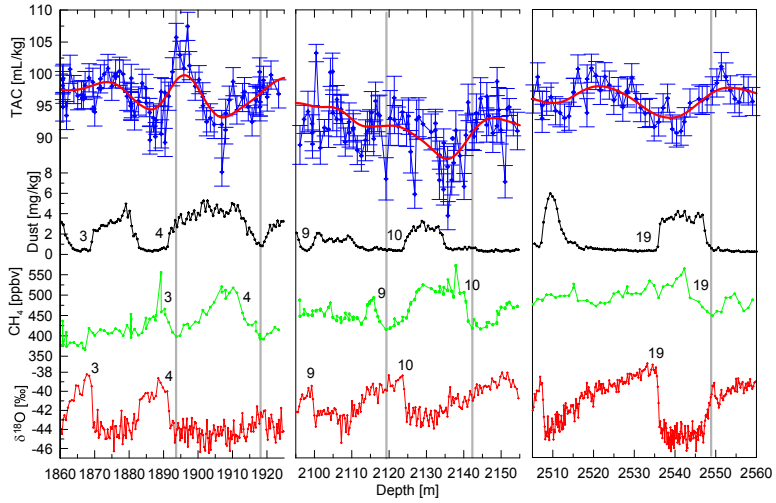

Figure 8. Zoom into DO-events 3 and 4, 9 and 10 and 19 on depth scale. In blue the TAC, including a spline with a 120 m COP (thick red line). In black the dust concentration (Ruth, 2007) in green the CH_4 and in red the $\delta^{18}O_{ice}$. Grey lines indicate the beginning of the DO-events in CH_4.

Discussion Paper | Discussion Paper | Discussion Paper | Discussion Paper |

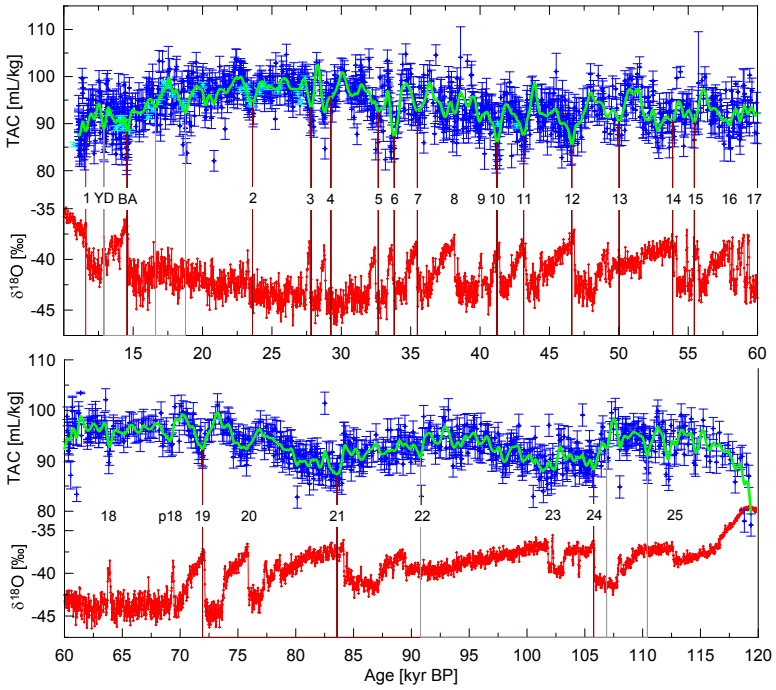

Figure 9. On top: the significant minima in the TAC spline with 750 yr COP from 10 to 120 kyr BP. The measured TAC on AICC2012 gas age scale in blue, the spline in green. Minima marked by ruby lines are considered significant by the algorithm described in the text, while significant minima without a close-by DO-event are indicated by grey lines. At the bottom the $\delta^{18}O_{ice}$ on the AICC2012 ice age scale.

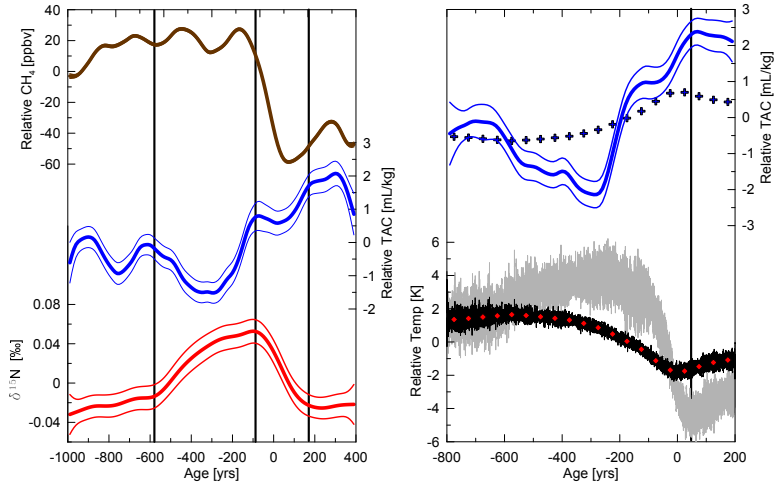

Figure 10. Stacked data over the onsets of all DO-events except DO-event 2 (Table 4). Left: in red the stacked δ^{15}N model data (Kindler et al., 2013), in blue the TAC and in brown the CH_4. Full lines represent the spline, thin lines the 1σ error range. Note that the variability in the stacked concentration only refers to the analytical error and not the variability between different DO-events. Grey lines indicate the start, the maximum and the end of the δ^{15}N signal. All three on AICC2012 gas age scale. Right: running mean over the modelled bubble close-off temperature (Kindler et al., 2013) in black, red squares indicate a 50 year mean. In grey the modelled surface temperature. Blue crosses represent the calculated TAC values dependent on bubble close-off temperature only. The blue lines represent the measured TAC on ice age scale. The black line indicates the onset of the surface temperature warming.

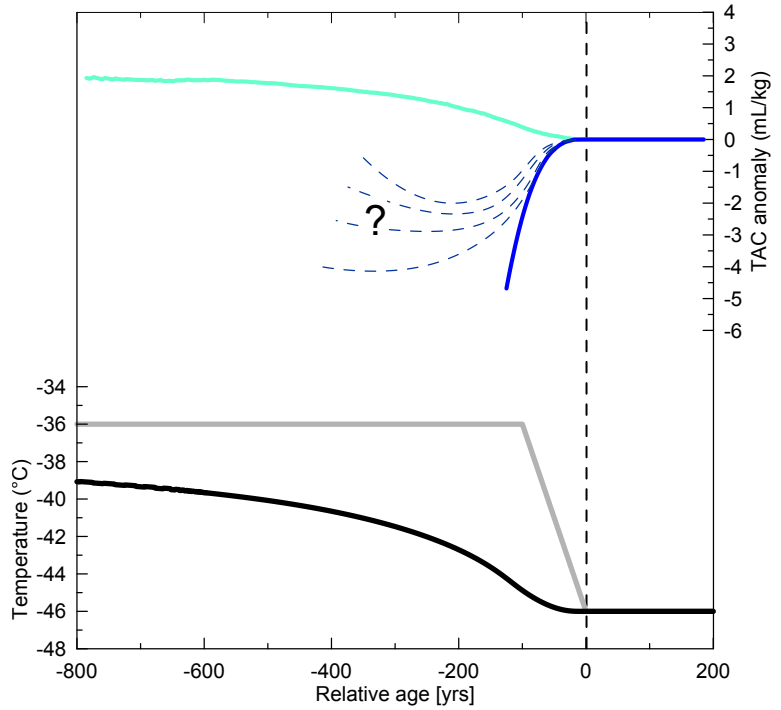

Figure 11. Modelled behaviour of TAC for a DO-event with a 10 °C surface warming during 100 years after the onset of the event. At the bottom, in grey the assumed surface temperature and in black the bubble close-off temperature. On top, in turquoise the TAC model output for steady state firnification conditions (Eq. 9). In blue the transient firnification model (Schwander et al., 1997) TAC output for a constant bubble-close-off time. Dashed blue lines indicate the range of measured TAC anomalies.